Design of boom expansion principle and luffing system of side - mounted tower crane

Lixia Meng, Kuiyuan Zhang, Bin Li *

Shenyang Jianzhu University, Shenyang, China

* Corresponding Author Email: 1834507661@qq.com

Abstract. In order to ensure normal movement and avoid interference in the erection and recovery process of the side-mounted rapid erection tower crane, our takes it as the research object, analyzes the structure composition and erection working principle of the boom part of the quick erection tower, and uses SolidWorks three-dimensional simulation to complete the drawing of different structure models of the tower crane. At the same time, the design of steel wire rope system is being studied, which provides a theoretical basis for the design of this kind of side-mounted tower crane.

Keywords: Side-mounted; Erection principle; Swing rope system Introduction.

1. Introduction

Compared with most rapid erection tower cranes, the side-mounted rapid erection tower crane studied by the author is divided into three sections. On the one hand, it can achieve a wider range of work. On the other hand, the lifting arm is placed on the side of the tower to reduce the height of the body. And in the folding process of the boom, in order to ensure that the luffing trolley can complete the normal luffing work under different states, the luffing wire rope system needs to be designed to ensure its normal work.

Therefore, I will specifically analyze the components and erection principle of the boom of this type of quick rack tower. At the same time, the paper studies the steel wire rope in different states, determines the distribution mode of pulley and puts forward the compensation design principle of steel wire rope with variable amplitude, as shown in Figure 1.

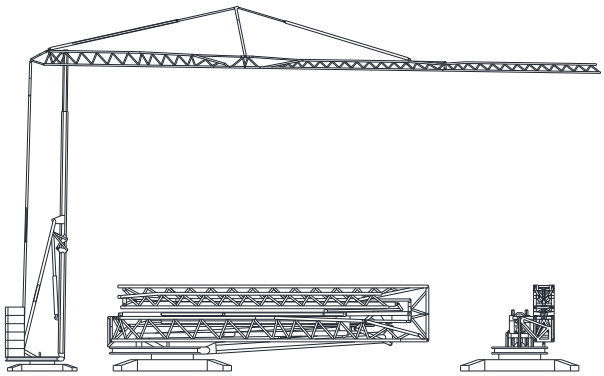


Figure 1. The working state of the tower crane and the front and side view of the transport state.

2. The Analysis Of Structure For Lift Arm

The overall composition of the lift arm part for the side-mounted tower crane see figure 2. It is composed of 1-the first arm, 2-the back tie rod, 3-the triangle connecting frame, 4-the front tie rod, 5-the second arm, 6-the third arm, 7-the folding hydraulic cylinder 3, 8-the folding hydraulic cylinder 2, 9-the arm connecting mechanism and 10-the folding hydraulic cylinder 1.

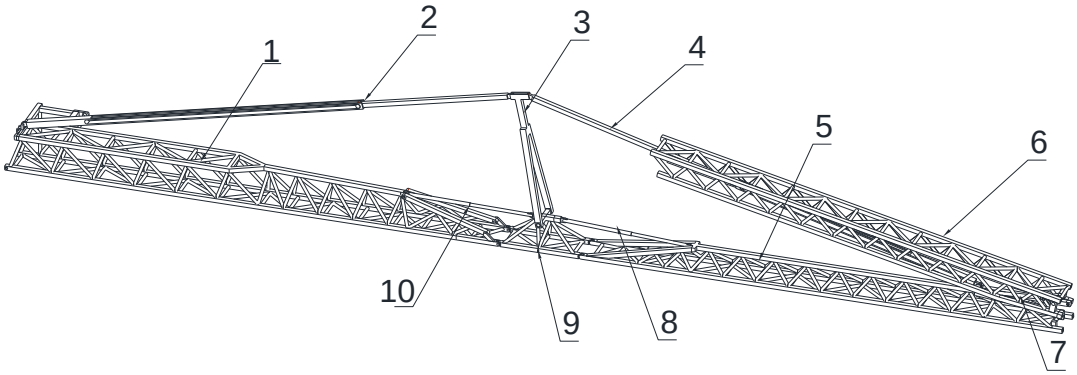


Figure 2. The structure for lift arm.

The lift arm part of the tower crane composed of three lifting arms is a truss structure. In order to realize the folding between the three lifting arms[1], the first and second arm are connected by the arm connecting structure in figure 3, and the bottom triangle connecting frame is joined the front and rear tie rod.

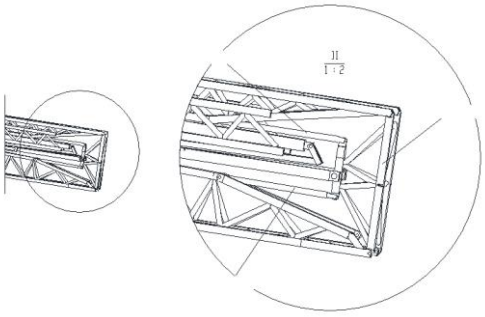


Figure 3. The connecting structure for the first arm and second arm

The second arm and the third arm are connected by the crank rocker structure and driven by the folding hydraulic cylinder to realize the 180 degree folding of the third arm in figure 4.

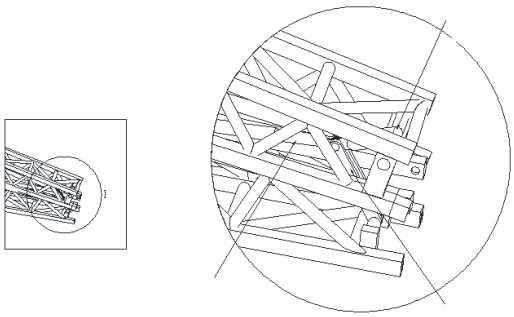


Figure 4. The connecting structure for the second arm and third arm

3. The Analysis Of Folding And Unfolding For Lift Arm

Different from other quick frame towers [2] [3], our studies the tower crane belongs to the side-mounted tower crane. The fold of the tower body and arm is realized in different stages, the upper tower and the lower tower stand up, and the inner tower body extends to achieve the expansion of the lift arm.

The lift arm for tower crane contains three sections and has four working states as shown in figure 5. State 1: After the tower body raises, the arm is unfolded and the second arm and third arm continue to be buckled above the first boom; State 2: The angle between the second arm and first arm gradually expands by driving the folding hydraulic cylinder 1 and folding hydraulic cylinder 2, and synergistic action the back tie rod and the front tie rod to realize expansion of the second arm; State 3: the third

arm expands through the folding hydraulic cylinder 3 is driven and the crank rocker mechanism works; State 4: The inner tower body continues to extend upward on the basis of the full expansion for three arm sections, and the whole arm is raised to a certain Angle around the connecting point of the tower body under the action of the boom tie rod [4].

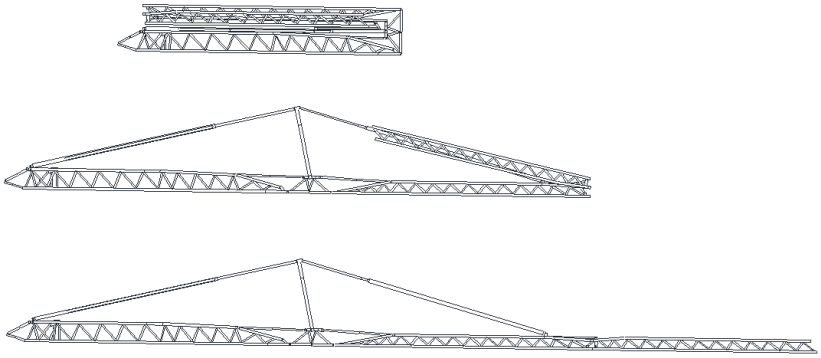


Figure 5. Four working states of the lift arm

4. The System Design Of Variable Amplitude Wire Rope

4.1. Variable Amplitude Principle

The content of the previous chapter explains the different working states of the lift arm, but the luffing trolley needs to complete normal work under different conditions, so the variable amplitude wire rope system is designed to meet the goal that the boom can complete different working states without readjusting the variable amplitude wire rope.

Figure 6 shows three different states of the tower crane and the winding diagram of the amplitude rope under different states. The amplitude system is composed of the amplitude driving mechanism 4, the luffing trolley 5, the guide rope pulleys of connector 6 and 7, the guide rope pulleys of folding arm 8, the double guide rope pulleys of folding arm 9, the guide rope pulleys of the arm end 10 and the variable amplitude wire rope 11.

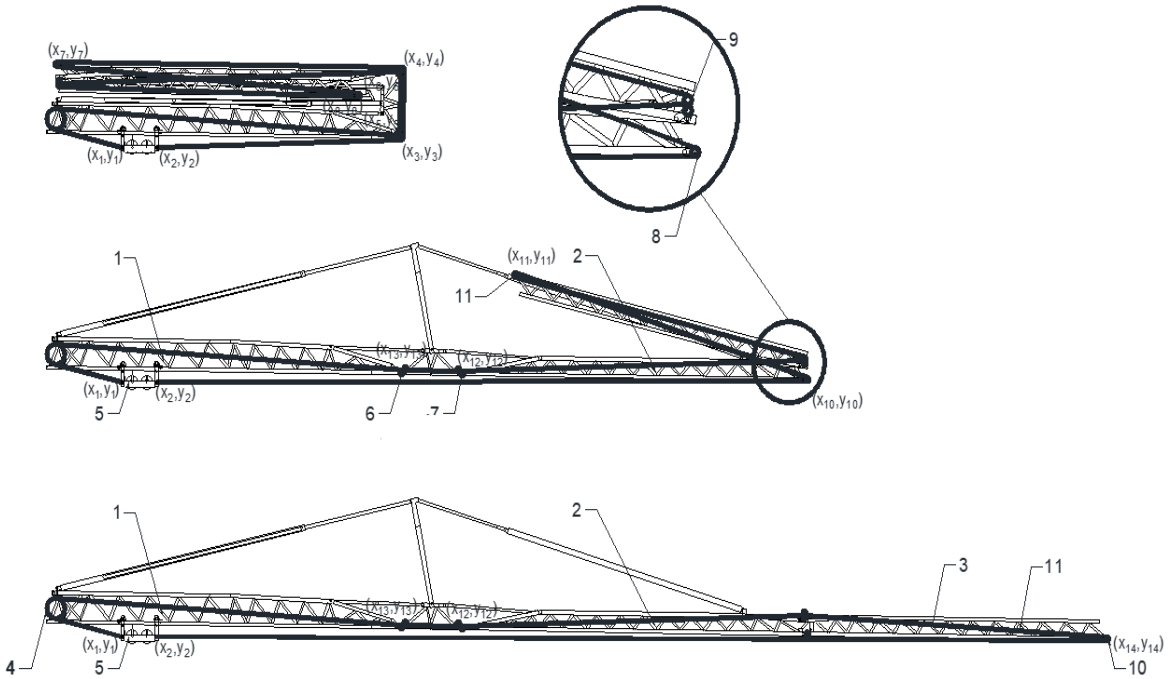


Figure 6. The winding diagram of variable amplitude wire rope.

The amplitude driving mechanism is installed at the root of the lifting arm, and the variable amplitude wire rope comes out of the reel. In state 3, the luffing trolley is connected and passes the guide rope pulleys of the arm end 10. However, when passing the connection of the second and third arm, due to the weight of the wire rope itself and the support of the guide rope pulleys of connector 6 and 7, it returns to the reel. When the third lifting arm returns to state 2, the working range of the luffing trolley is on the first and second lifting arm. It is wound to the guide rope pulleys of folding arm 8 of the folding arm through the steel wire rope extended by the trolley, and then enters the guide rope pulleys of the arm end 10 after changing direction. In the folding process, the steel wire rope changes from the double guide rope pulleys of folding arm 9 to the upper support of the winding pulley, and finally returns to the reel. Finally, after returning to state 1, the working range of the dolly is reduced to the first arm, and the winding of most guide rope pulleys remains unchanged, the wire rope extends from the upper part of the double guide rope pulleys of folding arm, and pass the guide rope pulleys of connector 6 and 7, then returns to the reel.

The total length of the variable steel rope before and after folding can change due to the constant change of winding mode of guide rope pulley during the folding process. Therefore, aiming to ensure the variable steel rope remains unchanged during the folding process and the normal operation of the variable steel rope, our studies the variation of variable rope and the layout of guide rope pulley in different states to provide a theoretical basis for this type of folding arm amplitude variation [5].

4.2. The design of Variable Amplitude Wire Rope

The layout of part of guide rope pulleys should be rationally selected to ensure the length of the variable rope is the same in state 1, state 2 and state 3 under the above method of wire rope winding. The following formula respectively analyzes the center coordinates of each guide rope pulleys in the three states [6].

The total length L_A of the luffing wire rope under state 1 is:

$$
\begin{cases}
L_A = l_a + l_b + l_c + l_d + l_e + l_f + l_g + l_h + l_i + l_{j_1} \\
l_a = \dfrac{x_1}{\cos\phi_1} + R_1 \cdot \tan\phi_1, l_b = \dfrac{x_3 - x_2}{\cos\phi_2} + R_2 \cdot \tan\phi_2 \\
l_c = y_4 - y_3, l_d = x_4 - x_7, l_e = \dfrac{x_8 - x_7}{\cos\phi_3} + 2R_2 \cdot \tan\phi_3 \\
l_f = \dfrac{x_8 - x}{\cos\phi_4} + 2R_2 \cdot \tan\phi_4, l_g = \dfrac{x_6 - x}{\cos\phi_5} + 2R_2 \cdot \tan\phi_5 \\
l_h = y_6 - y_5, x_5 = x_3 - a, y_5 = y_3 + b, x_6 = x_4 - a \\
y_6 = y_4 - b, l_i = \dfrac{x_5}{\cos\phi_6} - (R_1 + R_2) \cdot \tan\phi_6 \\
l_{j1} = \mathrm{R}_1(\pi - \phi_1 + \phi_6) + R_2(5\pi - \phi_2 - 2\phi_3 + \phi_6) \\
\phi_1 = \arctan\dfrac{y_1}{x_1} + \arcsin\dfrac{R_1}{\sqrt{x_1^2 + y_1^2}} \\
\phi_2 = \arctan\dfrac{y_3 - y_2}{x_3 - x_2} - \arcsin\dfrac{R_2}{\sqrt{(y_3 - y_2)^2 + (x_3 - x_2)^2}} \\
\phi_3 = \arccos\dfrac{2R_2}{\sqrt{(y_7 - y_8)^2 + (x_8 - x_7)^2}} - \arctan\dfrac{x_8 - x_7}{y_7 - y_8} \\
\phi_4 = \arccos\dfrac{2R_2}{\sqrt{(y_7 - y - h - y_8)^2 + (x_8 - x)^2}} \\
\quad - \arctan\dfrac{x_8 - x}{y_7 - y - h - y_8} \\
\phi_5 = \arccos\dfrac{2R_2}{\sqrt{(y_7 - y - h - y_6)^2 + (x_6 - x)^2}} \\
\quad - \arctan\dfrac{x_6 - x}{y_6 - y_7 + y + h} \\
\phi_6 = \pi - \arccos\dfrac{R_2 + R_1}{\sqrt{y_5^2 + x_5^2}} - \arctan\dfrac{x_5}{-y_5}
\end{cases}
\tag{1}
$$

In equation (1): x represents the horizontal distance between the vertical axis of the folding arm double guide rope pulley 9 and the sliding wheel of the connecting piece guide rope pulley 7; y represents the vertical distance from the horizontal axis of the folding arm double guide rope pulley 9 to the folding arm guide rope pulley 8; a represents the horizontal distance between the upper pulley and the sliding wheel of the connecting piece guide rope pulley 6; b represents the vertical distance between the upper pulley and the sliding wheel of the connecting piece guide rope pulley 6; R_1 is the radius of the reel; R_2 represents radius of the pulley 6, 7, 8, 9, 10; l_{j_1} represents the total length of the wire rope wound on the drum and the amplitude guide rope pulley.

The total length L_B of the luffing wire rope under state 2 is:

$$
\begin{cases}
L_B = l_k + l_l + l_m + l_n + l_o + l_p + l_q + l_{j2} \\
l_k = \dfrac{x_1}{\cos\phi_7} + R_1 \cdot \tan\phi_7, l_l = \dfrac{x_{10} - x_2}{\cos\phi_8} + R_2 \cdot \tan\phi_8 \\
l_m = \dfrac{x_{10} - x_{11}}{\cos\phi_9} \\
l_n = \dfrac{x + x_3 + y_4 - y_3 - x_{11}}{\cos\phi_{10}} + 2R_2 \cdot \tan\phi_{10} \\
l_o = \dfrac{x + x_3 + y_4 - y_3 - x_{12}}{\cos\phi_{11}} + R_2 \cdot \tan\phi_{11} \\
l_p = x_{12} - x_{13} + R_2(\tan\phi_{11} + \tan\phi_{12}) \\
x_{12} = x_3 + y_4 - y_3 - b, y_{12} = y_3 + a \\
x_{13} = x_3 + b, y_{13} = y_3 + a \\
l_q = \dfrac{x_{13}}{\cos\phi_{12}} - R_1 \tan\phi_{12} \\
l_{j2} = \mathrm{R}_1(\pi - \phi_7 + \phi_{12}) + R_2(3\pi - \phi_8 - 2\phi_9 + \phi_{12}) \\
\phi_7 = \arctan\dfrac{y_1}{x_1} + \arcsin\dfrac{R_1}{\sqrt{x_1^2 + y_1^2}} \\
\phi_8 = \arctan\dfrac{y_{10} - y_2}{x_{10} - x_2} - \arcsin\dfrac{R_2}{\sqrt{(y_{10} - y_2)^2 + (x_{10} - x_2)^2}} \\
\phi_9 = \arccos\dfrac{2R_2}{\sqrt{(y_{11} - y_{10})^2 + (x_{11} - x_{10})^2}} - \arctan\dfrac{x_{10} - x_{11}}{y_{11} - y_{10}} \\
\phi_{10} = \arccos\dfrac{2R_2}{\sqrt{(y + h - y_{11})^2 + (x_{11} - x)^2}} - \arctan\dfrac{x - x_{11}}{y_{11} - y - h} \\
\phi_{11} = \arctan\dfrac{x + x_3 + y_4 - y_3 - x_{12}}{y + h - y_{12}} \\
-\arcsin\dfrac{R_2}{\sqrt{(y + h - y_{12})^2 + (x_{12} - x - x_3 - y_4 + y_3)^2}} \\
\phi_{12} = \pi - \arccos\dfrac{R_2 + R_1}{\sqrt{y_{13}^2 + x_{13}^2}} - \arctan\dfrac{x_{13}}{-y_{13}}
\end{cases}
\tag{2}
$$

In equation (2): l_{j_2} represents the total length of the wire rope wound on the drum and the amplitude guide rope pulley.

The total length L_C of the luffing wire rope under state 3 is:

$$\begin{cases} L_C = l_r + l_s + l_t + l_u + l_v + l_w + l_{j3} \\ l_r = \dfrac{x_1}{\cos\phi_{13}} + R_1 \cdot \tan\phi_{13} \\ l_s = \dfrac{x_{14} - x_2}{\cos\phi_{14}} + R_2 \cdot \tan\phi_{14} \\ l_t = \dfrac{x_{14} - x - x_3 - y_4 + y_3}{\cos\phi_{15}} \\ l_u = \dfrac{x + x_3 + y_4 - y_3 - x_{12}}{\cos\phi_{16}} - R_2 \cdot \tan\phi_{16} \\ l_v = x_{12} - x_{13} + R_2(\tan\phi_{16} + \tan\phi_{17}) \\ l_w = \dfrac{x_{13}}{\cos\phi_{17}} - R_1 \tan\phi_{17} \\ l_{j3} = \mathrm{R}_1(\pi - \phi_{13} + \phi_{17}) + R_2(\pi - \phi_{14} + \phi_{17}) \\ \phi_{13} = \arctan\dfrac{y_1}{x_1} + \arcsin\dfrac{R_1}{\sqrt{x_1^{\,2} + y_1^{\,2}}} \\ \phi_{14} = \arctan\dfrac{y_{14} - y_2}{x_{14} - x_2} - \arcsin\dfrac{R_2}{\sqrt{(y_{14} - y_2)^2 + (x_{14} - x_2)^2}} \\ \phi_{15} = \dfrac{\pi}{2} - \arctan\dfrac{x_{14} - x - x_3 - y_4 + y_3}{y - y_{14}} \\ \phi_{16} = \arctan\dfrac{x + x_3 + y_4 - y_3 - x_{12}}{y - y_{12}} \\ \quad - \arcsin\dfrac{R_2}{\sqrt{(y - y_{12})^2 + (x + x_3 + y_4 - y_3 - x_{12})^2}} \\ \phi_{17} = \pi - \arccos\dfrac{R_2 + R_1}{\sqrt{y_{13}^{\,2} + x_{13}^{\,2}}} - \arctan\dfrac{x_{13}}{-y_{13}} \end{cases} \tag{3}$$

In equation (3): l_{j_3} represents the total length of the wire rope wound on the drum and the amplitude guide rope pulley.

At this time, let $L_A = L_B + L_C$, the position of folding double guide rope pulley x in (4) and the position of connecting piece guide rope pulley b in (5).

$$\begin{cases} x = \dfrac{(l_b + l_c + l_d + l_e + l_h + l_i + l_{j1} - l_{j2} - l_l - l_m - l_q)n}{u + v + w + m} \\ + \dfrac{e + f + g + i}{u + v + w + m} \\ u = \cos\phi_4 \cos\phi_{10} \cos\phi_{11} \\ v = \cos\phi_4 \cos\phi_5 \cos\phi_{10} \\ m = \cos\phi_4 \cos\phi_5 \cos\phi_{11} \\ w = \cos\phi_5 \cos\phi_{10} \cos\phi_{11} \\ n = \cos\phi_4 \cos\phi_5 \cos\phi_{10} \cos\phi_{11} \\ e = R_2(2u\sin\phi_5 + 2w\sin\phi_4 - 2v\sin\phi_{11} - 2m\sin\phi_{10} \\ -v\cos\phi_{11}\tan\phi_{12}) \\ f = (v + m)(y_3 - y_4 - x_3) \\ g = (x_4 - a)u + x_{11}m + x_8 w \\ i = v(x_{12} - x_{12}\cos\phi_{11} + x_{13}) \end{cases} \tag{4}$$

$$
\begin{cases}
b == \dfrac{\mu_1(l_b + l_c + l_d + l_e - l_h - l_i - l_{j1}) - \mu_2(l_s + l_v + l_w + l_{j3})}{\cos\phi_{15}(u+v+w+m)} \\
+ \dfrac{\mu_3 l_{j2} + \mu_4(l_l + l_m + l_p + l_q) + R_2 Z_1 + 2R_2 Z_2}{\cos\phi_{15}(u+v+w+m)} \\
+ \dfrac{x_3 s_2 - aqs_1 + t(x_{11}p + x_{12}o) + x_8 u - x_{14}v + w(q+r)(y_3 - y_4)}{\cos\phi_{15}(u+v+w+m)} \\
j = \cos\phi_4 \cos\phi_5 \cos\phi_{10} \cos\phi_{11} \cos\phi_{15} \\
k = \cos\phi_4 \cos\phi_5 \cos\phi_{10} \cos\phi_{11} \cos\phi_{16} \\
o = \cos\phi_4 \cos\phi_5 \cos\phi_{10} \cos\phi_{15} \cos\phi_{16} \\
p = \cos\phi_4 \cos\phi_5 \cos\phi_{11} \cos\phi_{15} \cos\phi_{16} \\
q = \cos\phi_4 \cos\phi_{10} \cos\phi_{11} \cos\phi_{15} \cos\phi_{16} \\
r = \cos\phi_5 \cos\phi_{10} \cos\phi_{11} \cos\phi_{15} \cos\phi_{16} \\
\mu_1 = k + o + p - j, \mu_2 = o + p + q + r, \mu_3 = q + r \mu_4 = j - k + q + r \\
s_1 = \dfrac{\cos\phi_5}{\cos\phi_{15}\cos\phi_{16}} + \dfrac{1}{\cos\phi_{15}} + \dfrac{1}{\cos\phi_{11}} + \dfrac{1}{\cos\phi_{10}} \\
s_2 = j(\dfrac{1}{\cos\phi_{11}} + \dfrac{1}{\cos\phi_{10}} - \dfrac{1}{\cos\phi_5} + \dfrac{2\cos\phi_{16}}{\cos\phi_5\cos\phi_{15}} + \dfrac{\cos\phi_{16}}{\cos\phi_4\cos\phi_{15}} \\
+ \dfrac{2\cos\phi_{16}}{\cos\phi_5\cos\phi_{11}} + \dfrac{2\cos\phi_{16}}{\cos\phi_5\cos\phi_{10}} + \dfrac{1}{\cos\phi_4\cos\phi_{11}} + \dfrac{1}{\cos\phi_4\cos\phi_{10}}) \\
t = \dfrac{1}{\cos\phi_{15}} - \dfrac{1}{\cos\phi_{16}} - \dfrac{1}{\cos\phi_5} - \dfrac{1}{\cos\phi_4} \\
u = r(\dfrac{1}{\cos\phi_{15}} - \dfrac{1}{\cos\phi_{16}} + \dfrac{1}{\cos\phi_{11}} + \dfrac{1}{\cos\phi_{10}}) \\
v = k(\dfrac{1}{\cos\phi_{11}} + \dfrac{1}{\cos\phi_{10}} + \dfrac{1}{\cos\phi_5} + \dfrac{1}{\cos\phi_4}) \\
w = \dfrac{1}{\cos\phi_{16}} - \dfrac{1}{\cos\phi_{15}} - \dfrac{1}{\cos\phi_{11}} - \dfrac{1}{\cos\phi_{10}} \\
z_1 = (\dfrac{o\sin\phi_{11}}{\cos\phi_{16}} - \dfrac{o\sin\phi_{11}}{\cos\phi_{15}} + \dfrac{p\sin\phi_{16}}{\cos\phi_{11}} + \dfrac{p\sin\phi_{16}}{\cos\phi_{16}} \\
+ \dfrac{q\sin\phi_{16}}{\cos\phi_{16}} + \dfrac{q\sin\phi_{11}}{\cos\phi_{11}} + \dfrac{r\sin\phi_{16}}{\cos\phi_{16}} + \dfrac{r\sin\phi_{11}}{\cos\phi_{11}}) \\
z_2 = (\dfrac{j\sin\phi_{10}}{\cos\phi_{10}} - \dfrac{j\sin\phi_5}{\cos\phi_5} - \dfrac{j\sin\phi_4}{\cos\phi_4} - \dfrac{k\sin\phi_{10}}{\cos\phi_{10}} \\
+ \dfrac{k\sin\phi_5}{\cos\phi_5} + \dfrac{k\sin\phi_4}{\cos\phi_4} + \dfrac{o\sin\phi_5}{\cos\phi_5} + \dfrac{o\sin\phi_4}{\cos\phi_4} \\
+ \dfrac{p\sin\phi_5}{\cos\phi_5} + \dfrac{p\sin\phi_4}{\cos\phi_4} + \dfrac{q\sin\phi_{10}}{\cos\phi_5} + \dfrac{q\sin\phi_{10}}{\cos\phi_4})
\end{cases}
\tag{5}
$$

4.3. The design principle of length compensator for amplitude rope

This section will introduce the dynamic changes of the variable amplitude wire rope caused by the arm folding action. The length calculation includes the following stages: the first stage is the third arm folded from the horizontal state to the steel wire rope is tangent to the pulley 8; the second stage is the arm continues to fold until the amplitude rope is tangent to the upper pulley of pulley 9; the third stage is to continue folding so that the third arm buckle on the second; the fourth stage is the overall upward folding until the amplitude variable wire rope is tangent to the sliding wheel of pulley 7, and then continue to fold to 90°; The fifth stage is the folding of the arm joint connector and the last two arms until the steel wire rope is tangent to the sliding wheel of pulley 6 and then the folding is completed.

1) The analysis of the length variation of the first stage

The length change of the amplitude variable wire rope can be expressed as follows:

$$\begin{cases} L_1 = l_r + l_s' + l_t + l_u + l_v + l_w + l_{j4} \\ l_s' = \sqrt{h_1^2 + R^2 - 2h_1 \cdot R \cdot \cos(\alpha + \beta) - R_2^2} \\ h_1 = \sqrt{(x_{15} - x_{10})^2 + (y_{15} - y_{10})^2} \\ h_2 = \sqrt{(x_{14} - x_{10})^2 + (y_{14} - y_{10})^2} \\ R = \sqrt{(x_{15} - x_{14})^2 + (y_{15} - y_{14})^2} \\ \alpha = \arccos \dfrac{h_1^2 + R^2 - h_2^2}{2h_1 \cdot R} \\ l_{j4} = \mathrm{R}_1(\pi - \phi_{13} + \phi_{17}) + R_2(\pi - \phi_{18} + \phi_{17}) \\ \phi_{18} = \arcsin \dfrac{R_2}{\sqrt{(y_{14}' - y_2)^2 + (x_{14}' - x_2)^2}} - \arctan \dfrac{y_{14}' - y_2}{x_{14}' - x_2} \end{cases} \tag{6}$$

l_r、l_t、l_u、l_v、l_w In (6) are the same as in (3).

2) The analysis of the length variation of the second stage

The length change of the amplitude variable wire rope can be expressed as follows:

$$\begin{cases} L_2 = l_r + l_{s1} + l_{s2} + l_t' + l_u + l_v + l_w + l_{j5} \\ l_{s1} = l_l \\ l_{s2} = \dfrac{x_{14}'' - x_{10}}{\cos \phi_{20}} \\ l_t' = \sqrt{h_3^2 + R^2 - 2h_3 \cdot R \cdot \cos(\theta + \alpha + \beta + \beta_1) - 4R_2^2} \\ h_3 = \sqrt{(x + x_3 + y_4 - y_3 - x_{15})^2 + (y + h - y_{15})^2} \\ \phi_{20} = \pi\text{-}\arctan \dfrac{y_{14}'' - y_{10}}{x_{14}'' - x_{10}} - \arccos \dfrac{2R_2}{\sqrt{(y_{14}'' - y_{10})^2 + (x_{14}'' - x_{10})^2}} \\ \phi_{21} = \pi\text{-}\arctan \dfrac{y_{14}'' - y_6}{x_{14}'' - x_6} - \arccos \dfrac{2R_2}{\sqrt{(y_{14}'' - y_6)^2 + (x_{14}'' - x_6)^2}} \\ (x_{14}'' - x_{15})^2 + (y_{14}'' - y_{15})^2 = R^2 \\ l_{j5} = \mathrm{R}_1(\pi - \phi_{13} + \phi_{17}) + R_2(\pi + \phi_{21} + \phi_{17}) \end{cases} \tag{7}$$

l_r、l_u、l_v、l_w In (7) are the same as in (3).

3) The analysis of the length variation of the third stage

The length change of the amplitude variable wire rope can be expressed as follows:

$$\begin{cases} L_3 = l_r + l_{s1} + l_{s2} + l_t + l_u + l_v + l_w + l_{j6} \\ l_{j5} = \mathrm{R}_1(\pi - \phi_{13} + \phi_{17}) + R_2(\pi + \phi_8 + \phi_{17}) \end{cases} \tag{8}$$

l_r、l_u、l_v、l_w In (8) are the same as in (3).

4) The analysis of the length variation of the fourth stage

The length change of the amplitude variable wire rope can be expressed as follows:

Pre-tangential: $L_4 = l_r + l_s' + l_t + l_u + l_v + l_w + l_{j7}$

Post-tangential: $L_4' = l_r + l_{s1}' + l_{s2}' + l_{s3}' + l_t + l_u + l_v + l_w + l_{j8}$

$$\begin{cases} l_s' = \sqrt{h_4^2 + R'^2 - 2h_4 \cdot R' \cos\alpha_1} \\ l_{s1}' = \dfrac{x_4 - x_2}{\cos\phi_{22}} + R_2 \cdot \tan\phi_{22} \\ l_{s2}' = \dfrac{x_{10}' - x_4}{\cos\phi_{23}} \\ l_{s3}' = l_{s2} \\ R' = \sqrt{(x_{10} - x_4)^2 + (y_{10} - y_4)^2} \\ h_4 = \sqrt{(x_4 - x_2)^2 + (y_4 - y_2)^2} \\ \phi_{22} = \arctan\dfrac{y_4 - y_2}{x_4 - x_2} - \arcsin\dfrac{R_2}{\sqrt{(y_4 - y_2)^2 + (x_4 - x_2)^2}} \\ \phi_{23} = \pi\text{-}\arctan\dfrac{y_{10}' - y_4}{x_{10}' - x_4} - \arccos\dfrac{2R_2}{\sqrt{(y_{10}' - y_4)^2 + (x_{10}' - x_4)^2}} \\ (x_{10}' - x_4)^2 + (y_{10}' - y_4)^2 = R'^2 \\ l_{j7} = \mathrm{R}_1(\pi - \phi_{13} + \phi_{17}) + R_2(\pi + \phi_8 + \phi_{17}) \\ l_{j8} = \mathrm{R}_1(\pi - \phi_{13} + \phi_{17}) + R_2(\pi + \phi_{22} + \phi_{17}) \end{cases} \tag{9}$$

5) The analysis of the length variation of the fifth stage

The length change of the amplitude variable wire rope can be expressed as follows:

Pre-tangential: $L_5 = l_r + l_{s1}'' + l_{s2}' + l_{s3}' + l_t + l_u + l_v + l_w + l_{j9}$

Post-tangential: $L_5' = l_r + l_{s1}''' + l_s''' + l_{s2}' + l_{s3}' + l_t + l_u + l_v + l_w + l_{j10}$

$$\begin{cases} l_{s1}'' = \sqrt{h_5^2 + R''^2 - 2h_5 \cdot R'' \cos\alpha_2} \\ l_{s1}''' = \dfrac{x_3 - x_2}{\cos\phi_{24}} + R_2 \cdot \tan\phi_{24} \\ l_s''' = y_4 - y_3 \\ R'' = \sqrt{(x_3 - x_2)^2 + (y_3 - y_2)^2} \\ h_5 = \sqrt{(x_3 - x_2)^2 + (y_3 - y_2)^2} \\ \phi_{24} = \arctan\dfrac{y_3 - y_2}{x_3 - x_2} - \arcsin\dfrac{R_2}{\sqrt{(y_3 - y_2)^2 + (x_3 - x_2)^2}} \\ (x_4' - x_3)^2 + (y_4' - y_3)^2 = R''^2 \\ l_{j9} = \mathrm{R}_1(\pi - \phi_{13} + \phi_{17}) + R_2(\pi + \phi_{22} + \phi_{17}) \\ l_{j10} = \mathrm{R}_1(\pi - \phi_{13} + \phi_{17}) + R_2(\pi + \phi_{24} + \phi_{17}) \end{cases} \tag{10}$$

5. Conclusions

We studied the structure of the lift arm of the side-mounted crane, the process of the expansion, and the three-arm folding system, and gave the calculation expression of the length of the steel wire rope in different states of the whole folding arm process to provide theoretical basis for determining the length of steel wire rope and length compensator in the future.

References

[1] G. P. Ghen, W. L. Luo, Y. Z. Guo, and X. Zheng, “Boom packing and stretching device of erected tower crane with three arms,” Design & Research, vol. 35, pp. 45-46+54, July 2014.

[2] C. W. Tian, and et al, “Dynamic Analysis of fast frame tower crane boom folding process,” Design & Research, vol. 36, pp. 39-41, June 2015.

[3] X. H. Li, and X. F. Li, “Structural Design of Jib of Folding Boom Truck Crane,” Modern manufacturing technology and equipment, vol. 58, pp. 42-46, April 2022.

[4] B. Lin, M. Zhai, “Design of variable amplitude steel wire rope system for fast erection of tower crane,” DESIGN & CALCULATION, vol. 498, pp. 64-69, August 2017.

[5] T. Huang, “Dynamic analysis of boom folding process of fast tower crane,” South forum, vol. 49, pp. 39, September 2018.

[6] C. R. GAO, and et al, “Multi-Objective Optimization of Variable Amplitude System for Mixing-Jib Overhead Working Truck,” Machinery Design & Manufacture, vol. 341, pp. 201-205+209, July 2019.